

Spin Dynamics of Rare Earth Ions in Phosphate Laser Glasses

I.P. Goudemon, J.M. Keartland, M.J.R. Hoch,
*Department of Physics, University of the Witwatersrand,
 P O WITS 2050, South Africa*

and G.A. Saunders
*School of Physics, University of Bath,
 Claverton Down, Bath BA2 7AY, UK*
 (July 15, 2021)

The spin dynamics of rare earth ions (Er, Nd, Sm and Gd) in heavily doped phosphate glasses have been investigated using ^{31}P NMR. Correlation times in the range 10^{-2} to 10^{-12} s have been obtained for temperatures between 4 K and 100 K. No evidence of spin-spin coupling between the ions has been found and spin relaxation occurs via conventional phonon processes, including the Orbach process.

A model involving inhomogeneous broadening of the NMR resonance lines, with distinct sample regions corresponding to the presence or absence of nuclear spin diffusion, has been used in extracting the electron spin correlation times from the NMR measurements.

PACS: 75.50.Kj. 76.30.Kg. 76.60.-k.

I. INTRODUCTION

Novel magnetic and magneto-optic phenomena, of interest for optoelectronic applications, have been found in the rare earth (R) metaphosphate glasses (REMG) with compositions in the vicinity $(\text{R}_2\text{O}_3)_{0.25}(\text{P}_2\text{O}_5)_{0.75}$. For example, these paramagnetic materials exhibit the largest known magnetic contributions to the low temperature specific heats in oxide glasses¹. X-ray diffraction and EX-AFS studies²⁻⁴ have shown that the structure of REMG comprises a 3-D network of corner-linked PO_4 tetrahedra, with the rare-earth ions, which in several instances are known to be trivalent R^{3+} , occupying sites within the PO_4 skeleton.

In recent work⁵, we have shown that it is possible to study the spin dynamics of rare earth ions in metaphosphate glasses using ^{31}P NMR as a probe. The present investigation has extended the NMR measurements to a number of REMG systems containing Er, Nd, Sm and Gd ions. For some of these systems, La or Y ions have been used as a buffer in order to lower the concentration of magnetic ions while preserving the metaphosphate glass structure. Information on the dynamics of the rare earth ions has been obtained using the model developed previously⁵.

II. THEORY

The local fields set up by paramagnetic ions lead to nuclear resonance frequency shifts and the establishment of an exclusion barrier of radius ρ_c , inside which spins are excluded from the observed NMR signal, together with a diffusion barrier of radius b_0 , inside which nuclear spin diffusion does not operate⁵. In highly paramagnetic systems of the type studied here, nuclear spin systems are thus composed of three distinct spatial regions corresponding to spin diffusive, non-diffusive and exclusion zones. The theory of nuclear spin lattice relaxation (NSLR) due to localized, isolated paramagnetic centres in magnetically dilute crystals⁶⁻¹¹ has been extended to account for magnetically concentrated systems⁵. In such systems, nuclear spin diffusion may be inoperative in appreciable fractions of sample volume, and nuclei may relax to multiple paramagnetic sites. The average relaxation rate for nuclei in diffusive regions is given by

$$\frac{1}{T_1} = \frac{4\pi}{3} n_s C^{\frac{1}{4}} D^{\frac{3}{4}} \quad (1)$$

in the diffusion limited [DL] case, and

$$\frac{1}{T_1} = \frac{4\pi}{3} \frac{n_s \gamma_I^{\frac{3}{2}}}{(\gamma_I \gamma_S \hbar)^{\frac{3}{2}} S^{\frac{3}{2}}} C \left(\frac{\Delta\omega}{\omega_n} \right)^{\frac{3}{4}} \left(\frac{k_B T}{3a_0} \right)^{\frac{3}{4}} \quad (2)$$

in the rapid diffusion [RD] case, with

$$C = \frac{2}{5} (\gamma_I \gamma_S \hbar)^2 S(S+1) \frac{\tau}{1 + \omega_n^2 \tau_e^2}. \quad (3)$$

D is the nuclear spin diffusion coefficient, n_s is the magnetic ion concentration and ω_n is the nuclear Larmor frequency⁵.

The net electronic relaxation rate for ions with a crystal field splitting includes direct, Raman and Orbach relaxation rates¹²⁻¹⁴:

$$\frac{1}{\tau_e} = \frac{1}{C_D \Delta^2} T + \frac{1}{C_R \Delta^2} T^7 + \frac{\Delta^3}{C_O} \frac{1}{\exp\left(\frac{\Delta}{k_B T}\right) - 1}. \quad (4)$$

C_D , C_R and C_O are relaxation constants for the direct, Raman and Orbach processes, respectively. Δ is the crystal field splitting.

In Gd^{3+} doped glasses, there is no crystal field splitting, and the ground state is a multiplet, so the net relaxation rate may be expressed as

$$\frac{1}{\tau_e} = \frac{1}{C_D} T + \frac{1}{C_R} T^5. \quad (5)$$

Equations 4 and 5 assume a Debye phonon density of states. This is consistent with recent work¹⁵, including the soft potential model approach, which suggests that vibrational modes in these systems are phonon-like. Fractons^{17,18} and 'excess' modes¹⁵ involving low-energy excitations do not appear to play a role in the relaxation processes in these systems.

III. EXPERIMENTAL DETAILS

The samples were prepared from the melt at Bath University with original stoichiometry²⁴ $(\text{R}_2\text{O}_3)_x(\text{X}_2\text{O}_3)_{.25-x}(\text{P}_2\text{O}_5)_{.75}$, and x in the range 0.01 to 0.25 (nominally), for $\text{R} = \text{Er}^{3+}$, Nd^{3+} , Sm^{3+} and Gd^{3+} , and $\text{X} = \text{Y}^{3+}$ or La^{3+} .

^{31}P NMR measurements at 8.5MHz (0.49 T) and 19.25MHz (1.1 T) were carried out using a pulsed NMR spectrometer and a Varian water-cooled electromagnet. Preliminary EPR measurements were carried out on Er and Gd REMG using a commercial X-band Bruker ESP380E pulsed EPR spectrometer and an Oxford continuous-flow helium cryostat to achieve low temperatures.

Nuclear resonance lineshapes have been characterised in terms of the moments of the resonance line determined from the Fourier Transform frequency-domain NMR spin-echo waveforms for samples with large inhomogeneous broadening.

The average nuclear relaxation rates for diffusive regions were extracted from the magnetization recovery data as a function of time τ using⁵

$$\frac{M(\tau)}{M_0} = 1 - 2\nu \left[f \cdot \exp\left(\frac{-\tau}{T_1}\right) + (1 - f) \cdot \exp\left(\frac{-\tau}{\lambda T_1}\right)^{\frac{1}{2}} \right], \quad (6)$$

where ν is a scaling factor, introduced because the degree of nuclear saturation is not known precisely, and f is the diffusive fraction of nuclei. The first and second terms describe NSLR in diffusive and non-diffusive regions, respectively. The relaxation rate for non-diffusive regions has been expressed in the form $T_1' = \lambda T_1$ for convenience, where λ is the ratio of the average relaxation rates for nuclei in diffusive and non-diffusive regions.

IV. RESULTS AND DISCUSSION

We were unable to observe EPR free induction decay or spin-echo signals in the samples investigated, probably due to extremely short spin-spin relaxation times

in these systems. Direct measurements of the electron spin-lattice relaxation time using pulsed EPR techniques have, therefore, not been possible.

Nuclear resonance lineshapes have been characterised in terms of the moments of the resonance line, using $\Delta\omega = \langle M_2 \rangle^{\frac{1}{2}}$, and the moment ratio, $R = \langle M_4 \rangle / \langle M_2 \rangle^2$. The NMR resonance line is inhomogeneously broadened due to coupling of the nuclear and paramagnetic ion moments. Fig. 1a shows plots of the inhomogeneously broadened ^{31}P nuclear resonance linewidth and moment ratio R versus inverse temperature for a 1% Er REMG at $B = 1.1$ T. The linewidth increases with decreasing temperature, eventually reaching a plateau at approximately 20 K. The ratio R is close to 3 at low temperatures, suggesting a characteristically Gaussian lineshape. The natural dipolar linewidth is estimated to be approximately 3.8 kHz, so there is appreciable inhomogeneous broadening of the linewidth even at the highest temperatures at which measurements were made. Following the onset of motional narrowing, R increases to around 5, implying a change in lineshape. This behaviour is typical of all the glasses studied. Fig. 1b shows plots of linewidth versus inverse temperature for various Er REMG samples. For each sample, the linewidth increases while the signal amplitude decreases with decreasing temperature, eventually becoming unobservably weak over a small temperature range. The signal-to-noise ratio increases with increasing resonance frequency so that, for a given sample, the temperature range over which the line can be observed is somewhat larger for a larger applied field.

It appears that the maximum observed linewidth depends on the magnetic ion concentration, the particular ion present and the magnetic field. In all cases, the NMR signal became immeasurably broad over a very small temperature range at sufficiently low temperatures. The relatively low maximum observed linewidth ($\Delta\omega < 25$ kHz) and the difference in maxima for different experiments strongly suggest that the abrupt loss of signal at low temperatures is not associated with limited spectrometer bandwidth. This loss of signal appears to be linked to the overlapping of diffusion barriers when two or more ions contribute to the line-broadening process for a majority of nuclear spins in all regions of the sample.

The ^{31}P spin-spin relaxation time, T_2 , determined from the spin-echo envelope, is 260 μs . For the Er^{3+} , Nd^{3+} and Sm^{3+} ion doped glasses, the electron correlation time approaches the nuclear T_2 value at temperatures in the vicinity of 5 K. For Gd^{3+} , the temperature at which τ_e becomes comparable to T_2 is approximately 50 K. When $\tau_e \lesssim T_2$, we expect the diffusion and exclusion barrier radii to reach their maximum values.

Fig. 2a shows plots of T_1^{-1} versus T^{-1} for the 1% Nd, 6% Nd and metaphosphate Nd REMG for $B = 4.9$ kG. The peak in the relaxation rate for the 1% Nd data corresponds to $\omega_n \tau_e = 1$. The temperature range over which measurements could be made on the 6% Nd and metaphosphate Nd REMG before the

line broadened dramatically rendering the signal unobservable, was insufficient to observe the peak. It is easily seen that the nuclear relaxation rate is proportional to the magnetic ion concentration, but it appears that the metaphosphate Nd REMG contains a magnetic ion concentration lower than the nominal 25%. The data have been analysed using Eq.1 [DL] and Eq.2 [RD]. The curves represent the best fits to the data of the [RD] and [DL] expressions. The Nd^{3+} data are well-described by the [RD] expression above 20 K, and follow the [DL] expression at lower temperatures. In Nd^{3+} , the contributions to electronic relaxation from the Raman and direct processes are negligible, and the data were analysed taking only the Orbach process into account for the temperature range covered in these experiments. All three Nd data sets were fitted using the same Orbach relaxation parameters. Both the lineshape data and the relaxation data provide no evidence that spin-spin interactions between the rare earth ions are important over the temperature range covered in the present experiment.

Fig. 2b shows plots of ${}^{31}\text{P}$ relaxation rates T_1^{-1} versus T^{-1} for the 1% Nd, 1% Er, and 20% Sm REMG. The nuclear relaxation rates for the Nd and Er REMG are similar at high temperatures. The peak in the Nd data occurs at a lower temperature than in the Er and Sm data. This suggests faster electronic relaxation in the Nd^{3+} ions, which results from a smaller crystal field splitting than in the other REMG. Nuclear relaxation in the 20% Sm REMG is much faster than in the Er and Nd REMG because of the much higher dopant concentration.

For the 1% Gd REMG, electronic relaxation is much less efficient than in the other REMG due to the absence of the Orbach process. The condition $\omega_n\tau_e = 1$ is not satisfied within the temperature range, and all the data are on the low temperature side of the relaxation peak (Fig. 2c). In Gd^{3+} , the whole data set is well described by the [DL] expression. The direct relaxation process dominates relaxation below 20 K, while the Raman process is most important at higher temperatures. Electronic relaxation parameters for Nd^{3+} , Er^{3+} , and Sm^{3+} ions appear in Table 1. For Gd^{3+} ions, the Orbach process is not operative and direct and Raman processes determine the ionic relaxation time. We obtain $C_D = 8.1(2) \times 10^{-2}(\text{s.K})$ and $C_R = 2.9(2) \times 10^5 (\text{s.K}^5)$ for the Gd^{3+} REMG.

The parameters listed in Table 1, together with C_R and C_D for Gd^{3+} , have been used to generate plots of the electronic relaxation rate τ_e^{-1} vs. T^{-1} for the magnetic ions studied (Fig. 3). It can be seen that the relaxation rates for ions with a crystal field splitting are much higher than for the Gd^{3+} ions. As noted above, it is clear from Fig. 2b that the relaxation behaviour of the 1% Nd and 1% Er glasses is very similar at higher temperatures. Fig. 3 shows that a crossover in electron correlation times for these two systems occurs at around 15 K.

The quality of the fits of the relaxation expressions to the experimental data and the consistency of the fitting parameters between data sets provide strong support for the model as well as for the use of electronic relaxation

expressions assuming a phonon density of states.

V. CONCLUSION

Measurements of the ${}^{31}\text{P}$ spin-lattice relaxation time in metaphosphate glasses doped with rare earth ions have provided information on the spin dynamics of these ions over a wide range of temperature. For Er, Nd and Sm ions, the observed behaviour with temperature is similar, with the spin correlation time being determined by a two-phonon Orbach process. The local environment of the ions is a distorted octahedron of oxygen atoms which give rise to crystal field splittings. Estimates of the splitting are provided by the present work for the ions mentioned above. In the case of Gd ions, where no crystal field splitting occurs, the paramagnetic ion correlation time is determined by direct and Raman processes. The approach we have established for determining details of paramagnetic ion behaviour in these systems should be widely applicable to similar systems.

¹ G. Carini, G. D'Angelo, G. Tripodo, A. Fontana, F. Rossi and G.A.Saunders, *Europhys. Lett.* **40**, 435 (1997).

² D.T. Bowron, R.J. Newport, B.D. Rainford, G.A. Saunders, and H.B. Senin, *Phys.Rev. B* **51**, 5739, (1995).

³ D.T. Bowron, G. Bushnell-Wye, R.J. Newport, B.D. Rainford and G.A. Saunders, *J.Phys.Condens.Matter* **8**, 3337 (1996).

⁴ Bowron, G.A. Saunders, R.J. Newport, B.D. Rainford and H.B. Senin, *Phys.Rev.* **53**, 5268 (1996).

⁵ I.P. Goudemond, J.M. Keartland, M.J.R. Hoch and G.A. Saunders, *Phys.Rev. B* **56**, R8463 (1997).

⁶ M. Goldman, *Spin Temperature and Nuclear Magnetic Resonance in Solids* (Oxford at the Clarendon, Oxford, 1970).

⁷ A. Abragam and M. Goldman, *Nuclear Magnetism: Order and Disorder* (Clarendon Press, Oxford, 1982).

⁸ H.E. Rorschach Jr., *Physica* **30**, 38 (1964).

⁹ G.R. Kutschvili, *Proc.Inst.Phys.Acad.Sci. Georgia (U.S.S.R.)* **4**, 3 (1956).

¹⁰ D. Tse and J. Lowe, *Phys.Rev.* **166**, 166 (1968).

¹¹ M.J. Duijvestijn, R.A.Wind and J. Smidt, *Physica* **138**, B 147 (1986).

¹² A. Abragam and B. Bleaney, *Electron Paramagnetic Resonance of Transition Ions* (Clarendon Press, Oxford, 1970).

¹³ C.B.P. Finn, R. Orbach and W.P. Wolf, *Proc.Phys.Soc. (London)* **77**, 261 (1961).

¹⁴ R. Orbach, *Proc.Roy.Soc. A* **264**, 485 (1961).

¹⁵ G. Carini, G. D'Angelo, G. Tripodo, A. Fontana, A. Leonardi, G.A. Saunders and A. Brodin, *Phys.Rev. B* **52**, 9342 (1995).

¹⁶ V.G. Karpov, M.I. Klinger and F.N. Igat'ev, *Sov.Phys.JETP* **57**(2), 439 (1983).

¹⁷ A.Fontana, F.Rocca and M.P.Fontana, Phys. Rev. Lett.

58, 503 (1987).

¹⁸ A.Aharony, S.Alexander, O.Entin-Wohlmann and R.Orbach, Phys. Rev. B **31**, 2565 (1985).

| | C_0 (s.K ⁵) | Δ (K) |
|------------------|---------------------------|--------------|
| Nd ³⁺ | $2.7(3) \times 10^{-7}$ | 88(5) |
| Er ³⁺ | $1.6(3) \times 10^{-7}$ | 102(5) |
| Sm ³⁺ | $1.1(3) \times 10^{-7}$ | 103(5) |

TABLE I. Electronic relaxation parameters for magnetic rare earth ions obtained from ^{31}P relaxation data. The quantities are defined in Eqs. (4) and (5)

FIG. 1. (a)Inhomogeneously broadened nuclear resonance linewidth (dots) and moment ratios (squares) for a 1% Er REMG with $B = 1.1$ T. (b)Inhomogeneously broadened nuclear resonance linewidths for 1% Er and 5% Er REMG with $B = 0.49$ T and $B = 1.1$ T.

FIG. 2. (a)Plots of T_1^{-1} versus T^{-1} for 1% Nd, 6% Nd and Metaphosphate Nd REMG. (b)Plots of T_1^{-1} versus T^{-1} for 1% Nd, 1% Er and 20% Sm. (c) A plot of T_1^{-1} versus T^{-1} for 1% Gd REMG. The curves are the best fits to the experimental data of the [RD] and [DL] expressions.

FIG. 3. Plots of the electronic relaxation rate extracted from nuclear relaxation data vs. inverse temperature for the magnetic rare earth ions studied.

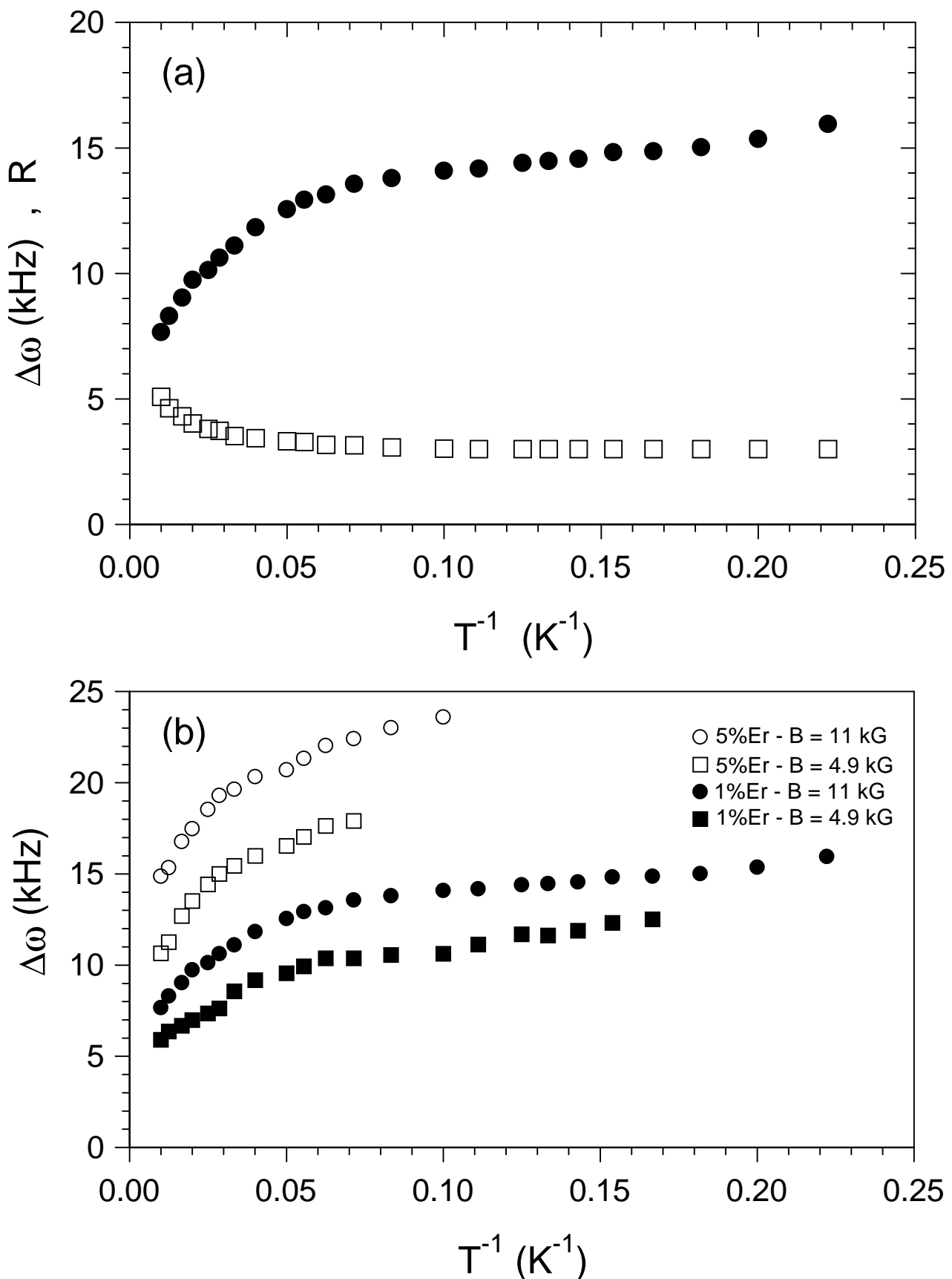


FIG 1

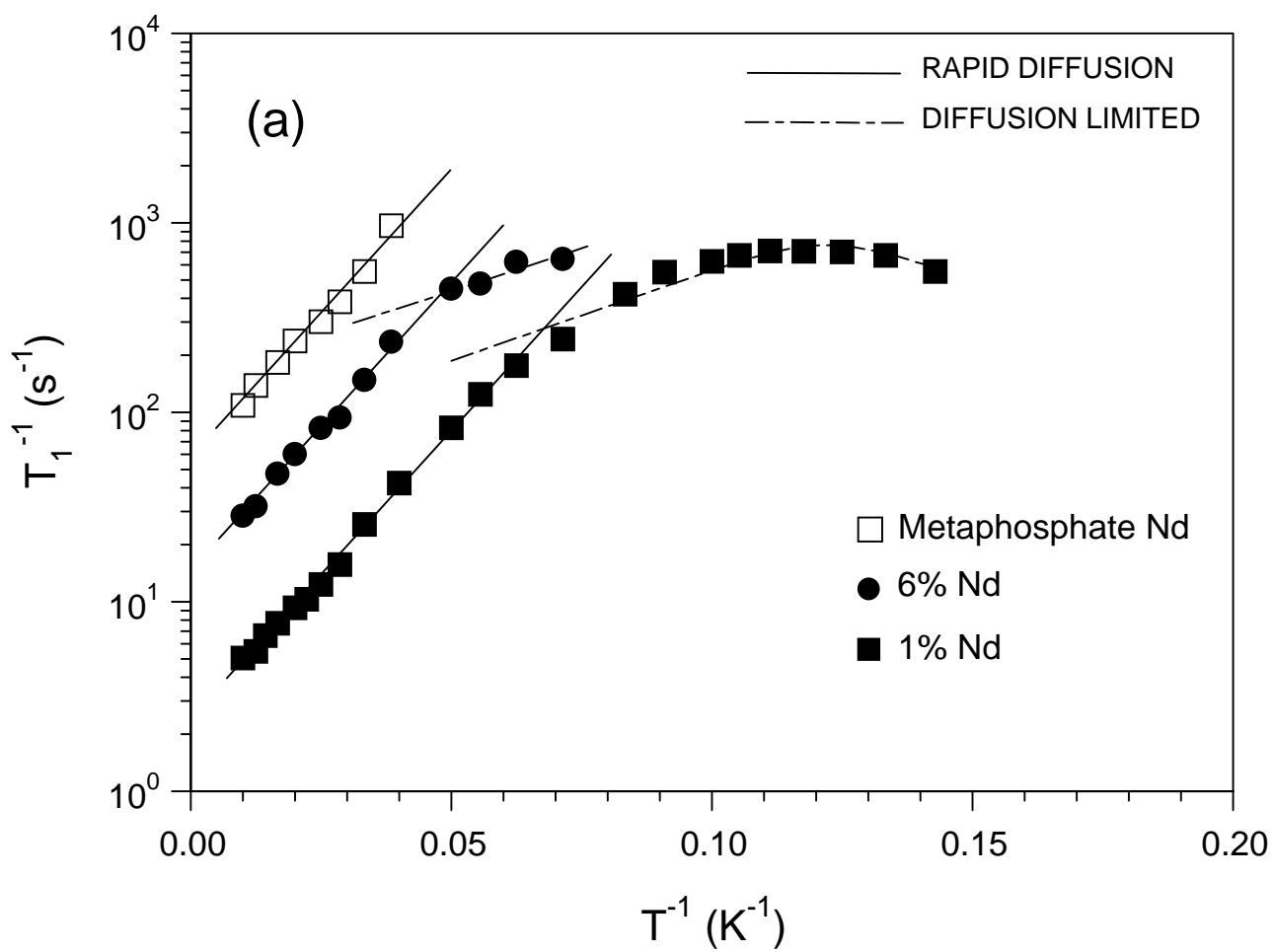


FIG 2a

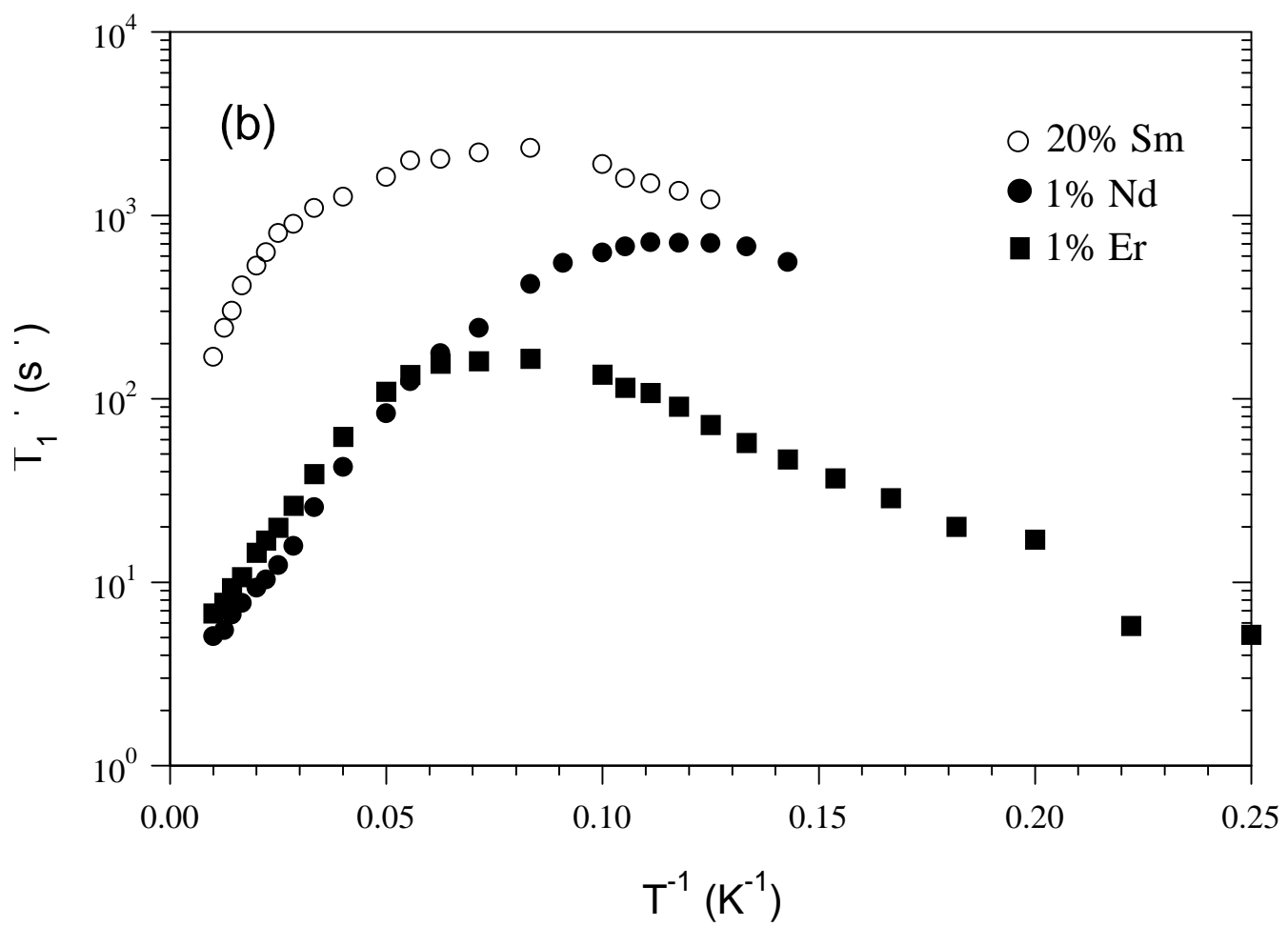


FIG 2b

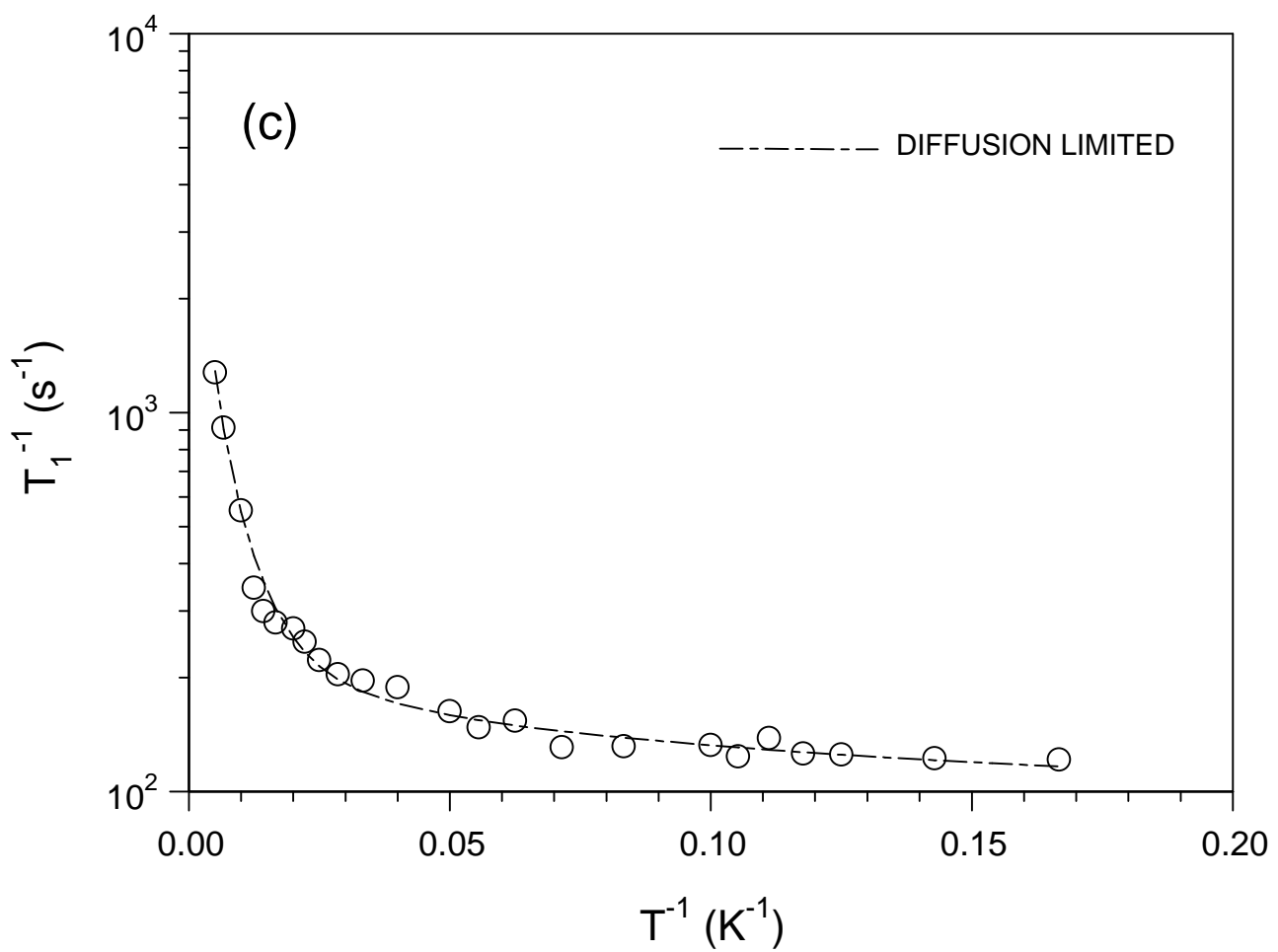


FIG 2c

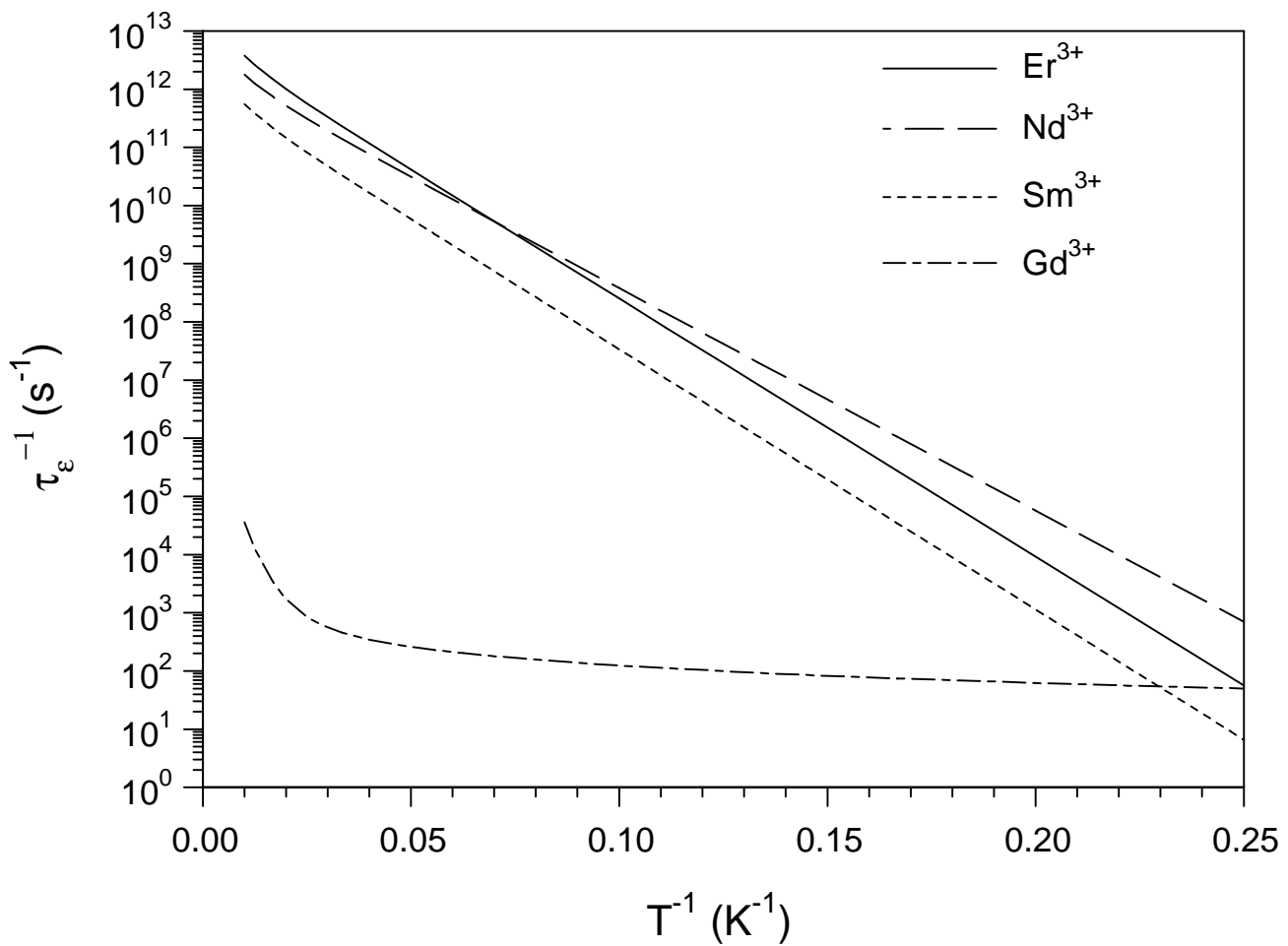


FIG 3